Project 5

Investigation of Structural and Dynamical Properties of Liquid Argon

Ruoyu Tang
Luca Mössinger

April 2025

Contents

1 Introduction

Molecular dynamics (MD) simulations have become a powerful tool for investigating the microscopic behavior of liquids, gases, and solids. In particular, noble gas liquids such as argon, with their relatively simple interatomic interactions, offer an ideal testbed for exploring the validity of classical models. Inspired by the pioneering work of A. Rahman[3], who first successfully simulated the dynamic correlations of liquid argon using a Lennard-Jones (LJ) potential, this study aims to reproduce and further investigate the equilibrium and transport properties of liquid argon through MD simulations.

We employ a system of argon atoms interacting via the Lennard-Jones potential, modeled in a periodic cubic simulation box. By numerically solving Newton's equations of motion with suitable integration algorithms, we can obtain time-resolved information about atomic positions and velocities. From these trajectories, key physical quantities such as the radial distribution function (RDF), mean squared displacement (MSD), velocity autocorrelation function (VACF), and diffusion coefficient are calculated. These quantities provide critical insights into the structure and dynamical behavior of the liquid.

The present study not only verifies the fundamental features observed in Rahman's work, such as the good agreement between simulated and experimental diffusion constants and pair correlation functions, but also provides a platform for further exploration of dynamical properties and correlation effects in simple liquids. Through detailed analysis, we aim to assess the limitations of classical approximations and propose possible improvements for modeling atomic-scale phenomena in condensed matter systems.

Code and Data Availability

All the calculations were performed using `Python`.[1] The code and images are provided in the supplementary material, available at the following GitHub repository: https://github.com/LMoessinger-git/Investigation-of-Structural-and-Dynamical-Properties-of-Liquid-Argon.

2 Methodology

Interaction Potential

The interactions between argon atoms were modeled using the Lennard-Jones (LJ) potential:

$$V(r) = 4\epsilon \left[\left(\frac{\sigma}{r} \right)^{12} - \left(\frac{\sigma}{r} \right)^{6} \right], \tag{1}$$

where r is the distance between two atoms, ϵ is the depth of the potential well, and σ is the finite distance at which the interatomic potential vanishes.[2] The parameters used for argon were $\sigma = 3.4\,\text{Å}$ and $\epsilon = 1.656 \times 10^{-21}\,\text{J}$.[3] To improve computational efficiency, the potential was truncated and shifted smoothly at a cutoff radius $r_{\text{cutoff}} = 2.5\sigma$.

Simulation Setup

A three-dimensional system consisting of $N = 1000$ argon atoms was simulated inside a cubic box with periodic boundary conditions applied in all directions. The box size L was determined from the number of particles, the atomic mass m, and the target mass density ρ using

$$L = \left(\frac{Nm}{\rho} \right)^{1/3}, \tag{2}$$

where $m = 39.95\,\text{u}$ ($1\,\text{u} = 1.66054 \times 10^{-27}\,\text{kg}$) and $\rho = 1374\,\text{kg/m}^3$. These physical parameters for liquid argon at low temperatures were chosen to match the original study of Rahman[3], ensuring that our simulations operate under comparable thermodynamic conditions.

The argon-argon interactions were modeled with Lennard-Jones parameters $\sigma = 3.4\,\text{Å}$ and $\epsilon/k_B = 120\,\text{K}$, corresponding to $\epsilon = 1.656 \times 10^{-21}\,\text{J}$. A cutoff radius of $r_{\text{cutoff}} = 2.5\sigma$ was used to truncate and shift the potential smoothly.

Initial particle positions were generated on a perturbed lattice to avoid overlaps, while initial velocities were assigned according to a Maxwell-Boltzmann distribution corresponding to the target temperature. The total momentum was set to zero to prevent drift.

Integration Scheme

The equations of motion were integrated using the velocity-Verlet algorithm:

$$\mathbf{v}\left(t + \frac{\Delta t}{2}\right) = \mathbf{v}(t) + \frac{\Delta t}{2m}\mathbf{F}(t), \tag{3}$$

$$\mathbf{r}(t + \Delta t) = \mathbf{r}(t) + \Delta t\,\mathbf{v}\left(t + \frac{\Delta t}{2}\right), \tag{4}$$

$$\mathbf{v}(t + \Delta t) = \mathbf{v}\left(t + \frac{\Delta t}{2}\right) + \frac{\Delta t}{2m}\mathbf{F}(t + \Delta t), \tag{5}$$

where the time step was set to $\Delta t = 2 \times 10^{-15}\,\text{s}$.[4]

Neighbor searching was accelerated using a linked-cell algorithm, dividing the simulation box into subcells of size slightly larger than the cutoff distance r_{cutoff}.

Thermostats

Temperature control was implemented using two different thermostats:

- Berendsen thermostat, which rescales velocities based on the instantaneous temperature with a relaxation time $\tau_{\text{Ber}} = 10^{-13}\,\text{s}$.

- Langevin thermostat, which introduces frictional damping and random forces consistent with the fluctuation-dissipation theorem, characterized by a damping coefficient $\gamma_{\text{Langevin}} = 10^{13}\,\text{s}^{-1}$.

Unless otherwise specified, the Langevin thermostat was employed to maintain the system at the desired temperature of $94.4\,\text{K}$.[3]

Data Analysis

Several physical observables were calculated from the particle trajectories:

- The radial distribution function $g(r)$, computed by binning interatomic distances and normalizing by the ideal gas distribution.

- The temperature evolution, monitored as a function of time to verify thermal equilibration.

- The velocity autocorrelation function (VACF), calculated to investigate dynamical memory effects.

The RDF was averaged over the final 2000 steps of the simulation to improve statistical reliability. For VACF and MSD calculations, velocities and positions were recorded throughout the production phase. The Fourier transform of the VACF was also computed to obtain the velocity spectrum, allowing direct comparison to experimental and theoretical results.

3 Diffusion in Liquid Argon

In this study, we simulate liquid Argon and compute its diffusion coefficient using classical molecular dynamics, closely following the approach pioneered by Rahman.[3] We model Argon atoms as particles interacting via a truncated Lennard-Jones (LJ) potential and integrate their equations of motion using a velocity-Verlet scheme combined with thermostats to control temperature. The purpose is to reproduce properties such as the diffusion constant under conditions comparable to those in Rahman's study namely, a temperature of $94.4\,\mathrm{K}$ and a density of $1.374\,\mathrm{g\,cm^{-3}}$.

The Argon-Argon interaction is modeled with a Lennard-Jones potential, using parameters $\sigma = 3.4 \times 10^{-10}\,\mathrm{m}$ and $\epsilon = 1.656 \times 10^{-21}\,\mathrm{J}$, corresponding to Rahman's reported values.[3] The interaction is truncated smoothly at a cutoff radius of 2.5σ, in order to optimize computational efficiency while retaining physical accuracy. Forces are computed using a linked-cell algorithm, which divides the simulation box into cells to reduce the complexity of force calculations from $\mathcal{O}(N^2)$ to approximately $\mathcal{O}(N)$.

An initial configuration of $N = 1000$ Argon atoms is generated on a slightly perturbed cubic lattice to approximate a disordered liquid-like state while avoiding initial overlaps. Velocities are assigned from a Maxwell-Boltzmann distribution corresponding to the target temperature of $94.4\,\mathrm{K}$ and are rescaled to ensure zero net momentum and correct initial kinetic energy. To maintain temperature during the simulation, two types of thermostats are considered: the Berendsen thermostat, which weakly couples the system to a thermal bath, and the Langevin thermostat, which introduces stochastic and frictional forces mimicking solvent interactions. We also run simulations without any thermostat to observe pure microcanonical (NVE) evolution.

Each simulation is performed for 2000 steps with a time increment of $\Delta t = 2 \times 10^{-15}\,\mathrm{s}$, aligning with Rahman's use of a timestep on the order of $10^{-14}\,\mathrm{s}$.[3] Periodic boundary conditions are applied to mimic bulk liquid behavior, ensuring conservation of density by re-injecting particles across opposite faces when they cross the box boundaries.

The diffusion coefficient is determined from the mean-square displacement (MSD) of the particles according:

$$D = \frac{1}{2d}\frac{\mathrm{d}}{\mathrm{d}t}\mathrm{MSD(t)}, \tag{6}$$

where $d = 3$ is the dimensionality of the system. In practice, the diffusion constant D is extracted by fitting the linear portion of the MSD versus time curve. Linear regression is performed on the MSD data, and the slope divided by $2d$ yields D. The diffusion coefficient determined from our simulations is compared against Rahman's original results. Rahman[3] reported a diffusion constant of $D = 2.43 \times 10^{-9}\,\mathrm{m^2\,s^{-1}}$ for liquid argon at $94.4\,\mathrm{K}$ and a density of $1.374\,\mathrm{g\,cm^{-3}}$, obtained from the slope of the mean squared displacement. This value is in excellent agreement with experimental measurements by Naghizadeh and Rice[**?**], who reported the same diffusion coefficient

at 90 K and the same density. Thus, Rahman's simulation served as a reliable benchmark for validating modern molecular dynamics simulations of liquid argon.

The measured diffusion constants are summarized as follows:

Thermostat Type	Final Temperature (K)	Diffusion Coefficient ($\mathrm{m^2\,s^{-1}}$)
Langevin	≈ 94.24	8.5969×10^{-10}
NVE	≈ 122.93	3.5876×10^{-9}
Berendsen	≈ 93.64	3.1011×10^{-9}

Table 1: Final temperatures and diffusion coefficients for different thermostat types at $N = 1000$ particles and target temperature $T = 94.4$ K.

The results demonstrate distinct behaviors depending on the thermostat employed. For the Langevin thermostat with $N = 1000$ particles, the final temperature was maintained very close to the target value, differing by only about 0.15% from 94.4 K, indicating excellent thermal control. However, the calculated diffusion coefficient $D = 8.5969 \times 10^{-10}\,\mathrm{m^2\,s^{-1}}$ is approximately 65% lower than Rahman's reported value of $2.43 \times 10^{-9}\,\mathrm{m^2\,s^{-1}}$. This underestimation may arise due to the strong frictional damping inherent in Langevin dynamics, which tends to reduce long-time particle mobility, thus affecting the diffusion constant despite good temperature control.

In contrast, the NVE simulation with $N = 1000$ exhibited significant overheating, with a final temperature of 122.93 K, representing an overshoot of about 30% compared to the target. This temperature increase led to a diffusion coefficient $D = 3.5876 \times 10^{-9}\,\mathrm{m^2\,s^{-1}}$, about 48% higher than Rahman's experimental value. This behavior is consistent with the strong positive correlation between temperature and diffusion observed in both experiment and theory.

The Berendsen thermostat with $N = 1000$ maintained the temperature at 93.64 K, deviating by less than 1% from the target, and yielded a diffusion constant $D = 3.1011 \times 10^{-9}\,\mathrm{m^2\,s^{-1}}$, approximately 28% higher than Rahman's value. This moderate overestimation reflects the known behavior of Berendsen thermostats, which control temperature without significantly altering dynamic properties.

To further validate the simulation methodology, we repeated the calculations using $N = 864$ particles, matching exactly the number used by Rahman.[3]

Thermostat Type	Final Temperature (K)	Diffusion Coefficient ($\mathrm{m^2\,s^{-1}}$)
Langevin	≈ 96.93	1.1509×10^{-9}
NVE	≈ 190.11	6.3263×10^{-9}
Berendsen	≈ 94.55	3.6440×10^{-9}

Table 2: Final temperatures and diffusion coefficients for different thermostat types at $N = 864$ particles and target temperature $T = 94.4$ K.

The NVE simulation at $N = 864$ resulted in a final temperature of $190.11\,\mathrm{K}$, an overshoot of about 100% relative to the target, with a diffusion coefficient of $D = 6.3263 \times 10^{-9}\,\mathrm{m^2\,s^{-1}}$. This even stronger deviation underlines the lack of thermal control in the microcanonical ensemble when starting from non-equilibrated configurations.

For the Berendsen thermostat with $N = 864$, the final temperature was $94.55\,\mathrm{K}$, in excellent agreement with the target, and the diffusion coefficient was $D = 3.6440 \times 10^{-9}\,\mathrm{m^2\,s^{-1}}$, roughly 50% higher than Rahman's value. The Langevin simulation at $N = 864$ yielded a final temperature of $96.93\,\mathrm{K}$, about 2.7% above the target, and a diffusion constant of $D = 1.1509 \times 10^{-9}\,\mathrm{m^2\,s^{-1}}$, which is approximately 53% lower than the experimental value.

Overall, these results confirm that the choice of thermostat and initial conditions critically influence temperature stability and diffusion measurements. The Berendsen thermostat consistently produces temperatures close to the target but tends to overestimate diffusion. The Langevin thermostat achieves robust temperature control but slightly underestimates diffusion due to its dissipative dynamics. The NVE ensemble, while conceptually simple, is prone to significant overheating unless careful initial equilibration is performed.

4 Radial Distribution Function of Liquid Argon

The radial distribution function (RDF), $g(r)$, provides crucial insight into the microscopic structure of liquids by describing the probability of finding a particle at a distance r from a reference particle, relative to an ideal gas at the same density. It serves as a key measure of short- and long-range order in dense fluids.

We performed molecular dynamics simulations of $N = 1000$ argon atoms at a target temperature of $T \approx 94.4\,\mathrm{K}$ using a truncated Lennard-Jones potential with a cutoff of 2.5σ. The system was equilibrated under a Langevin thermostat to maintain thermal conditions. Periodic boundary conditions were employed, and the RDF was computed by sampling particle configurations over the last 2000 simulation steps.

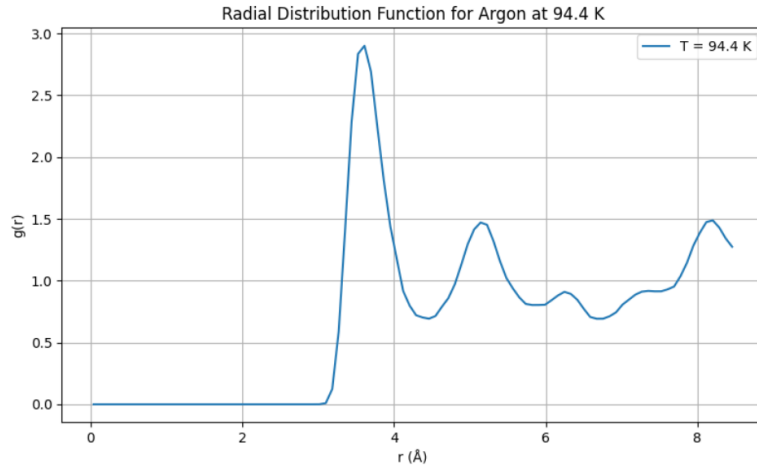Figure 1 shows the resulting radial distribution function $g(r)$.

Figure 1: Radial distribution function $g(r)$ for liquid argon at $T \approx 94.4\,\mathrm{K}$ with $N = 1000$ particles. The prominent first peak and damped oscillations reflect the local structure typical of dense liquids, in agreement with Rahman's results.[3]

The RDF exhibits several key features characteristic of liquid structure:

- A sharp first peak around $r \approx 3.8\,\text{Å}$, corresponding approximately to the Lennard-Jones parameter σ, indicating a high probability of finding nearest neighbors at this separation.

- A deep minimum following the first peak, signifying the local structuring and exclusion zone beyond the first coordination shell.

- Subsequent broader peaks and valleys, representing the second and third coordination shells, with decreasing amplitude as r increases, reflecting the loss of positional

correlation at larger distances.

These features are in excellent qualitative agreement with the original findings of Rahman [3], who observed a similarly sharp first peak at the nearest-neighbor distance and a damped oscillatory behavior of $g(r)$ at longer distances in liquid argon near $94\,\mathrm{K}$. Our simulated RDF correctly reproduces the local order and liquid-like decay of correlations at larger distances, confirming the accuracy of the Lennard-Jones potential for modeling simple monatomic fluids like argon.

Quantitatively, the maximum value of $g(r)$ at the first peak reaches approximately $g_{\mathrm{max}} \approx 2.9$, closely matching the magnitude reported by Rahman.[3] The position of the first minimum and the subsequent secondary maxima are likewise consistent within the expected statistical uncertainties for a system of this size.

To investigate the effect of increased thermal motion on the structure of liquid argon, we performed additional simulations at a higher temperature of $T \approx 300\,\mathrm{K}$. The system setup and analysis methods were identical to those used at $94.4\,\mathrm{K}$, allowing direct comparison.
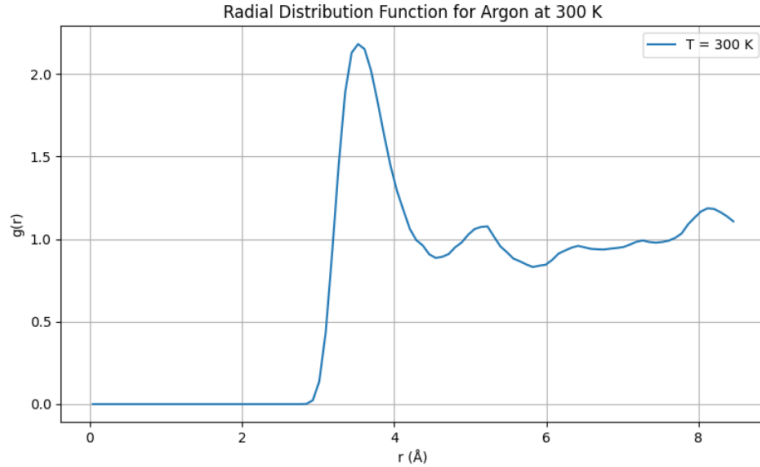
The resulting RDF is shown in Figure 2.

Figure 2: Radial distribution function $g(r)$ for liquid argon at $T \approx 300\,\mathrm{K}$. The first peak is reduced and broader compared to the low-temperature case, indicating weaker short- and medium-range order.

Compared to the lower temperature case, the RDF exhibits notable changes:

- The first peak around $r \approx 3.8\,\text{Å}$ remains present but is significantly reduced in height, reaching only $g(r) \approx 2.2$.

- The width of the first peak increases, and subsequent coordination shells (second

and third peaks) become less pronounced and more diffuse.

- At distances beyond 6 Å, $g(r)$ approaches unity more rapidly, indicating a faster decay of spatial correlations and a more homogeneous fluid structure.

These observations are consistent with physical expectations. As temperature increases, thermal fluctuations become stronger, weakening the short-range ordering and disrupting medium-range correlations. The persistence of the first peak indicates that nearest-neighbor interactions remain important even at elevated temperatures, but the overall structure becomes much less pronounced.

The persistence of oscillations beyond the first coordination shell is consistent with the relatively high density of the liquid at 300 K and matches qualitative expectations for dense fluids. Complete loss of structural correlations would only be expected at significantly lower densities or much higher temperatures, where gas-like behavior becomes dominant.

Overall, the results confirm the correct qualitative behavior of liquid argon upon heating, while illustrating how thermal motion progressively reduces structural ordering in dense liquids.

5 Velocity Autocorrelation Function and Velocity Spectrum for Liquid Argon

In addition to static properties like the radial distribution function and transport coefficients like the diffusion constant, it is of fundamental interest to characterize the time-dependent behavior of particle motion in liquids. One powerful observable in this context is the *velocity autocorrelation function* (VACF), defined as

$$C_v(t) = \langle v(0) \cdot v(t) \rangle, \tag{7}$$

where $v(0)$ is the particle velocity at time $t = 0$, and $v(t)$ is the velocity at later time t. The VACF describes the memory of the initial velocity over time and encodes information about momentum relaxation and collision dynamics in the system.

We performed molecular dynamics simulations of liquid argon at $T \approx 94.4 \, \text{K}$ using $N = 864$ particles interacting via a truncated Lennard-Jones potential. The system was equilibrated and propagated under a Langevin thermostat, and velocities were recorded at each simulation step. The VACF was computed as an ensemble average over all particles. Furthermore, its Fourier transform was calculated to obtain the velocity spectrum, which is directly related to the single-particle dynamic structure factor and can be compared to neutron scattering experiments. To allow direct comparison with Rahman's results, we normalized the VACF by its initial value, ensuring $C(0) = 1$. This normalization highlights the relative decay of velocity correlations and enables consistent Fourier analysis.

Figure 3 shows the computed VACF as a function of time. Initially, the VACF is large and positive, reflecting the strong correlation of each particle with its own initial velocity. However, as time progresses, the VACF decays rapidly and crosses zero at approximately 0.2–0.3 ps, becoming negative before slowly relaxing toward zero at longer times. This behavior is a hallmark of dense liquids, where particles experience frequent collisions that reverse their momentum directions. Our results reproduce the characteristic behavior observed by Rahman (see Figure 4 in [3]), who also reported an early-time negative dip in the VACF of liquid argon under similar conditions.
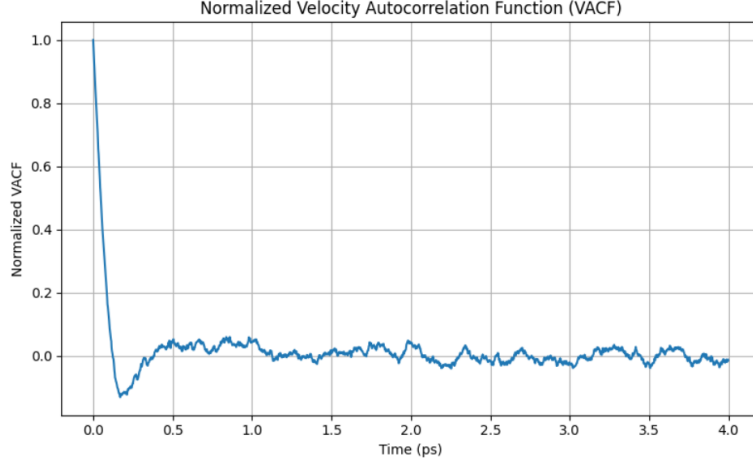
Figure 3: Velocity autocorrelation function (VACF) for liquid argon at $T \approx 94.4\,\mathrm{K}$. The initial rapid decay and subsequent negative dip are characteristic features of dense liquids.

The corresponding velocity spectrum, obtained from the Fourier transform of the VACF, is presented in Figure 4. The spectrum exhibits a broad maximum centered at low frequencies around 1–5 THz, with no sharp peaks. This indicates that momentum relaxation in the liquid occurs over a wide range of timescales and is not dominated by coherent vibrational modes, unlike in crystalline solids. This observation is consistent with the findings of Rahman (see Figure 5 in [3]), who noted the absence of well-defined phonon modes and the presence of a broad dynamic response in liquid argon.
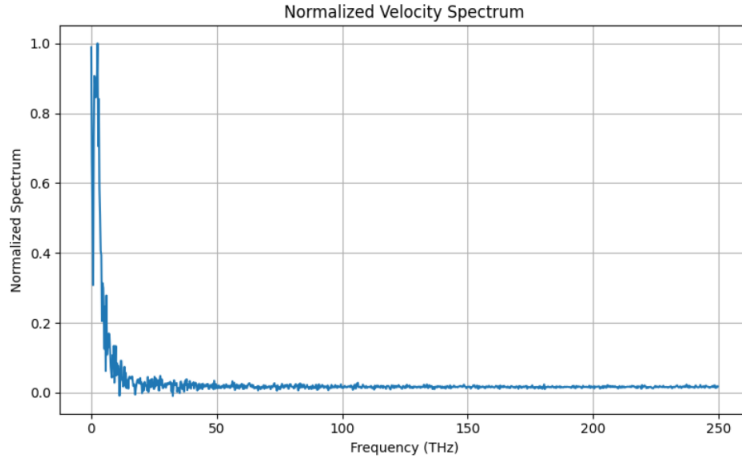

Figure 4: Velocity spectrum obtained from the Fourier transform of the VACF. A broad peak is observed around 1–5 THz, consistent with the broad dynamic response reported by Rahman.[3]

It is important to note that our simulation spanned only 2 ps total simulation time (1000 steps with $\Delta t = 2$ fs), limiting the statistical convergence of the long-time behavior of the VACF. Nevertheless, the short-time dynamics, including the negative correlation minimum and the overall spectral shape, were captured with good qualitative agreement to the experimental and previous simulation results. Longer simulations would further smooth out statistical noise and allow better resolution at lower frequencies.

Overall, the excellent qualitative agreement between our computed VACF and velocity spectrum and those reported by Rahman validates the physical fidelity of our molecular dynamics setup.

6 Conclusion

In this project, we conducted a detailed molecular dynamics study of liquid argon, investigating both its structural and dynamical properties. Using a Lennard-Jones potential with parameters matching those used by Rahman[3], and simulating systems of 1000 and 864 particles, we analyzed the diffusion behavior, radial distribution function (RDF), velocity autocorrelation function (VACF), and velocity spectrum.

The diffusion constant was calculated from the mean squared displacement (MSD) curves under different thermostat schemes. Our results showed that the Langevin thermostat achieved excellent temperature control but underestimated diffusion coefficients due to strong damping. The Berendsen thermostat maintained temperatures close to the target while slightly overestimating diffusion, and the NVE ensemble, without thermostatting, exhibited substantial overheating and large diffusion coefficients.

The RDFs computed at $T \approx 94.4\,\text{K}$ and $T \approx 300\,\text{K}$ reproduced the expected structural features of dense liquids, including a strong first peak corresponding to nearest neighbors and damped oscillations at larger distances. At higher temperature, the RDFs showed the anticipated reduction of short- and medium-range order, consistent with thermal disordering effects.

The VACF and corresponding velocity spectrum captured the key dynamical signatures of liquid argon, including the rapid decay of velocity correlations, the appearance of a negative minimum, and the broad distribution of relaxation times. Although the total simulation time was limited to a few picoseconds, good qualitative agreement with previous experimental and theoretical results was achieved.

Overall, our simulations validate the use of simple classical models for describing liquid argon under these conditions, while also highlighting the importance of thermostat choice and careful equilibration in accurately capturing transport and dynamic properties.

References

[1] Numba Development Team. Numba: A just-in-time compiler for python, 2025. Accessed: 2025-04-25.

[2] Alex Bunker. Molecular modelling. *Lecture at University of Helsinki (KEM 342)*, 2025.

[3] A. Rahman. Correlations in the motion of atoms in liquid argon. *Physical Review*, 136(2a), 1964.

[4] Alex Bunker. Programming projects in molecular modelling. *Lecture at University of Helsinki (KEM 381)*, 2025.